



Removal of metronidazole antibiotic by modified red mud from aqueous solutions: process modeling, kinetic, and isotherm studies

Fatemeh Lotfi Golsefidi¹ · Mohaddeseh Zahmatkesh Anbarani¹ · Ziaeddin Bonyadi²

Received: 6 November 2022 / Accepted: 9 August 2023 / Published online: 15 September 2023
© The Author(s) 2023

Abstract

Metronidazole is a type of antibiotic that is commonly used to treat bacterial infections in both humans and animals. The objective of this study was to eliminate MDZ from aqueous solutions using MRM. To gain a better understanding of the adsorption mechanism, we utilized kinetic and isotherm models to investigate the factors that affect the removal of MDZ. The Box–Behnken model was utilized to design experimental factors, which included the initial concentration of MDZ (ranging from 5 to 80 mg/L), MRM dose (ranging from 0.1 to 0.7 g/L), reaction time (ranging from 10 to 60 min), and pH (ranging from 4 to 10). Analysis of the adsorbent using FESEM, FTIR, EDX, DLS, and zeta potential provided valuable insights into its morphology, surface properties, functional groups, size, and electrical charge. Acid modification of red mud increased the porosity and number of pores on the adsorbent surface, thereby enhancing its ability to adsorb the MDZ antibiotic. The FTIR spectrum displays various bands corresponding to different functional groups, such as O–H, Si(Al)–O, Fe–O, and carbonate groups. EDX analysis revealed that the composition of MRM includes carbon, oxygen, and nitrogen elements. The DLS and zeta potential data demonstrate the impact of particle size and electric charge of the adsorbent on the removal of MDZ. The maximum removal of MDZ, which was 69.87%, was achieved at an MDZ concentration of 42.5 mg/L, a pH of 7, a contact time of 35 min, and an adsorbent dose of 0.4 g/L. The removal of MDZ follows both the pseudo-second-order model and the Langmuir model. The maximum adsorption capacity was found to be 6.04 mg/g. The findings of this study indicate that MRM successfully removes MDZ from aqueous solutions.

Keywords Antibiotic · Metronidazole · Red mud · Adsorption · Box–Benken mode

Abbreviations

MDZ	Metronidazole
MRM	Modified red mud
FT-IR	Fourier-transform infrared spectroscopy
pHzpc	Zero point of charge
FESEM	Field emission scanning electron microscopy

ANOVA	Analysis of variance
BBD	Box–Benken design

Introduction

A variety of compounds are slowly becoming prominent as contaminants that enter aquatic bodies through municipal and industrial wastewater (Gondi et al. 2022). These include pesticides, disinfectant byproducts, and antibiotics (Pirsaheb et al. 2013; Esmaili et al. 2023). According to the World Health Organization, 25% of water pollution is attributed to pharmaceutical products. With the rapid growth of the population and the development of agriculture, various types of antibiotics have been produced (Weidner et al. 2021). The widespread use of antibiotics can lead to allergic reactions, adverse effects, and the development of antibiotic-resistant microorganisms (Li et al. 2022). Antibiotics exist in surface water, groundwater, sewage, drinking water, and food

Fatemeh Lotfi Golsefidi and Mohaddeseh Zahmatkesh Anbarani have contributed equally to this work as Co-first author.

✉ Ziaeddin Bonyadi
Bonyadiz@mums.ac.ir

¹ Student Research Committee, Department of Environmental Health Engineering, School of Health, Mashhad University of Medical Sciences, Mashhad, Iran

² Department of Environmental Health Engineering, School of Health, Mashhad University of Medical Sciences, Mashhad, Iran

products (Juella 2021). Even at low concentrations, these pollutants have a negative effect on the environment, ecosystem, human health, and drinking water quality (Hena et al. 2020). Certainly, antibiotics have revolutionized modern medicine and are effective in treating bacterial infections. However, they can also have negative effects on health. One of the most significant concerns regarding antibiotics is the emergence of antibiotic resistance. Overusing antibiotics can result in the development of antibiotic-resistant bacteria that are difficult to treat and can quickly spread. This can lead to serious infections that are difficult to treat and may even be life-threatening (Esmaili et al. 2023). Antibiotics can disrupt the natural balance of bacteria in the gut. The gut harbors a complex ecosystem of microorganisms that play a crucial role in digestion and overall health. Antibiotics can disrupt the delicate balance of microorganisms in the gut, potentially leading to digestive problems such as diarrhea, as well as other health issues. Some individuals may also develop allergic reactions to specific antibiotics (Zahmatkesh Anbarani et al. 2023). MDZ is an antibiotic used for treating infections (Sepehr et al. 2017). Due to its high solubility and poor biodegradability, this antibiotic is commonly found in water bodies (Fang et al. 2011).

Common treatment methods are ineffective in removing antibiotics from urban and industrial wastewaters. Therefore, these pollutants enter the water environment in large quantities (Berges et al. 2021). Today, researchers are exploring new techniques to eliminate emerging pollutants and mitigate their toxic effects on aquatic environments (Ighalo et al. 2020). Various techniques have been employed to remove different antibiotics, including ion exchange resin (Wang et al. 2017), electrocoagulation (Zhou et al. 2022), ozonation (Nasuhoglu et al. 2012), advanced oxidation processes (Lima et al. 2020), membrane technology (Nasrollahi et al. 2022), and ultrafiltration (Li et al. 2022). Adsorption-based processes are more interesting compared to other techniques because of their advantages, such as high efficiency, low cost, availability, profitability, and ease of operation (Gu et al. 2019). These processes are typically effective in eliminating various pollutants from water-based solutions (Juella 2021). RM generally consists of oxides and hydroxides of aluminum, silica, iron, calcium, and titanium (Wang et al. 2005). RM has been used to remove various environmental pollutants (Tor et al. 2006). Tandekar et al. (2021) effectively removed several anions, including phosphate, chromate, and fluoride ions, using a combination of red mud and chitosan (Tandekar et al. 2021). In previous studies, RM has been utilized to eliminate phenol (Tor et al. 2009), copper (Nadaroglu et al. 2010), and trace elements (da Conceição et al. 2021). RM is a mixture of metal oxides that acquires a positive charge through hydroxylation in aqueous environments (Aydin et al. 2019). Given the abundance of red mud and the valuable materials it contains, the primary objective

of this research is to explore the use of red mud as an efficient and cost-effective adsorbent for removing MDZ from water environments. The research findings were analyzed using Langmuir, Freundlich, and Temkin isotherms, as well as pseudo-first-order, pseudo-second-order, and intraparticle diffusion kinetics. The study investigated the impact of various factors, such as pH, contact time, adsorbent dose, and initial MDZ concentration, on the removal efficiency.

Materials and methods

Materials

Metronidazole with a purity of 99% was purchased from Dana Pharmaceutical Company in Iran. RM was purchased from Alumina Company in Iran. All chemicals were obtained from Merck in Germany. Double-distilled water was used to prepare all solutions.

Preparation of red mud

Initially, RM was treated with 1N nitric acid for 24 h. The modified RM was then washed with distilled water to remove any excess acid, dried at 150 °C for 4 h, and sifted through a 100 mesh sieve (Shirzad-Siboni et al. 2014).

Characteristics The characteristics of MRM particles were investigated by FTIR, FESEM, EDX, DLS, and zeta potential tests.

Preparation of reaction mixtures

MDZ removal was performed under different laboratory conditions. To prepare for laboratory experiments, we first created a stock solution of MDZ at a concentration of 100 mg/L. This was achieved by dissolving 0.1 g of MDZ powder in 1000 mL of distilled water. The main laboratory factors, including contact time (10–60 min), pH (4–10), initial MDZ concentration (5–80 mg/L), and MRM dose (0.1–0.7 g/L), were investigated. Sodium hydroxide solution and sulfuric acid were used to adjust the pH of the samples. Table 1 displays the range of primary parameters utilized for MDZ removal. The samples were stirred using a shaker

Table 1 Range of key parameters for MDZ removal

Factor	Variable level			
	Code	−1	0	+1
MDZ Conc. (mg/L)	A	5	42.5	80
Contact time (min)	B	10	35	60
Red mud (g/L)	C	0.1	0.4	0.7
pH	D	4	7	10

at a speed of 300 rpm. After completing the tests, 10 cc samples were collected from the laboratory solutions. These samples were then centrifuged for 10 min at 5000 rpm to separate the adsorbent from the suspension. The resulting supernatant was filtered through a 0.22 μm filter. Finally, the concentration of MDZ in suspension was measured using a spectrophotometer at λ_{max} of 320 nm. The MDZ removal rate can be calculated using the formula (Zambrano et al. 2021; Mpelane et al. 2022):

$$\text{MDZ removal (\%)} = \frac{(C_0 - C_e) \times 100}{C_0} \quad (1)$$

where C_0 represents the initial concentration of MDZ (mg/L) and C_e represents the concentration of MDZ in the treated solution after a specified period of time.

$$q_e = \frac{(C_0 - C_e)}{m} \times V \quad (2)$$

The equation is as follows: W/V = mass of red mud (in grams) divided by the volume of the reaction mixture (in liters).

Adsorption kinetic and isotherm studies

Adsorption kinetics can be used to investigate the reaction rate, the variables that affect the reaction rate, and the transport behavior of the particles of the adsorbed substance. To achieve this goal, a reaction mixture was prepared with a concentration of 20–80 mg/L of MDZ, a contact time of 5–60 min, a pH of 5, and an MRM dose of 2.5 g/L. After conducting the tests, the removal rate of MDZ was assessed. Kinetic equations, such as the pseudo-first-order, pseudo-second-order, and intraparticle diffusion models, were calculated (Bonyadi et al. 2023). In the next step, adsorption isotherms were measured to describe how the amount of solute affects the adsorbent. For this purpose, the study results were evaluated using Langmuir, Freundlich, and Temkin adsorption isotherms (Bonyadi et al. 2022a, b).

Langmuir isotherm

Langmuir's isotherm is applicable when the surface is monolayer and homogeneous adsorption occurs. The Langmuir isotherm is as follows (Bonyadi et al. 2022a, b):

$$\frac{C_e}{Q_e} = \frac{1}{b \times Q_{\text{Max}}} + \frac{C_e}{Q_{\text{Max}}} \quad (3)$$

In this formula, Q_{max} is the maximum sorption capacity (mg/g), Q_e is the equilibrium sorption capacity, and b is the Langmuir constant (L/mg) (Bonyadi et al. 2022a, b).

Freundlich isotherm

The effects of several variables, including the heterogeneity and energies of active sites following an exponential distribution, are assumed through an experimental model (Yoosefian et al. 2017). Freund The Freundlich isotherm is as follows:

$$\ln q_e = \ln k + \frac{1}{n} \ln C_e \quad (4)$$

In this formula, q_e represents the adsorption capacity at equilibrium (mg/g), while k_f denotes the Freundlich constant (L/g) (Nasoudari et al. 2021).

Results and discussion

Characterization

FESEM FESEM analysis was used to evaluate the morphology and surface characteristics of the adsorbent. Figure 1a–b indicates FESEM images of RM and MRM. The FESEM image displays RM particles with an agglomerated and slightly rough surface (Fig. 2a). After modifying the red mud with acid (Fig. 2b), the porosity and pores on the adsorbent surface are significantly increased. This modification enhances the adsorption capacity of the material, allowing it to effectively capture more MDZ antibiotic.

FTIR FTIR was used to analyze and identify the functional groups present on the surface of the adsorbent. The results of the FTIR analysis are shown in Fig. 2. Focusing on Fig. 2a, we can see that the FTIR spectrum comprises various bands. The following bands are observed at the corresponding wavenumbers: 432 cm^{-1} , 571 cm^{-1} , 686 cm^{-1} , 878 cm^{-1} , 998 cm^{-1} , 1119 cm^{-1} , 1433 cm^{-1} , 1629 cm^{-1} , 1797 cm^{-1} , 3433 cm^{-1} , and 3530 cm^{-1} . The band observed in the range of 3433–3530 cm^{-1} is associated with O–H groups. The peaks observed at 998 cm^{-1} , 443 cm^{-1} , and 1433 cm^{-1} correspond to Si(Al)–O, Fe–O, and carbonate groups, respectively (Smičiklas et al. 2013). After the acidic modification of RM, a strong band at 1415 cm^{-1} was observed due to the stretching of the C=O bond. However, this band was reduced by the dissolution of CaCO_3 caused by the addition of acid to RM (Deihimi et al. 2018). The spectrum of RM showed the absence of Al–O and Fe–O bonds, possibly due to the dissolution of Fe and Al oxides/hydroxides (Fig. 2b). After the removal of MDZ, the C=C bond shifted to 1570 cm^{-1} as shown in Fig. 3C. (Theamwong et al. 2021).

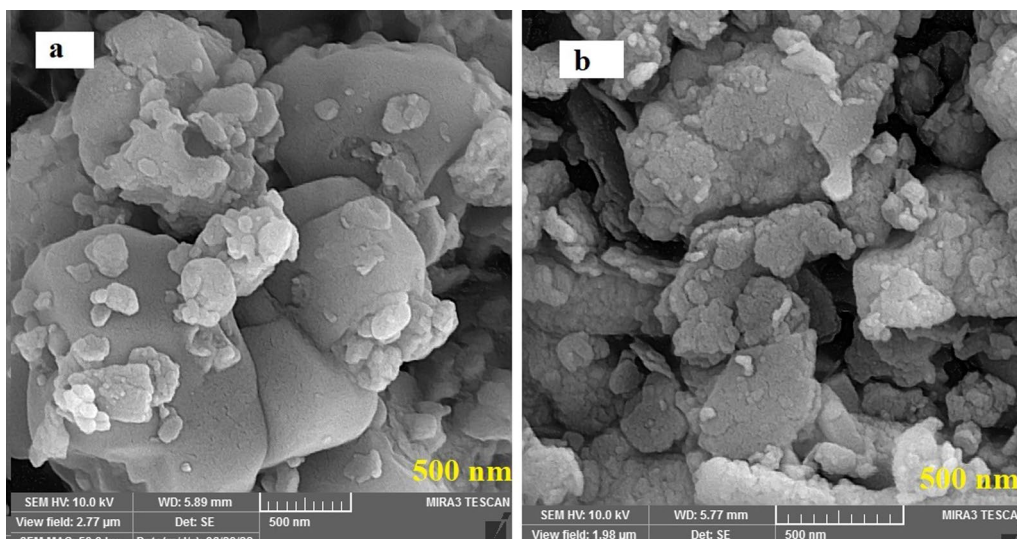


Fig. 1 FESEM images of mud red (a) and modified mud red (b)

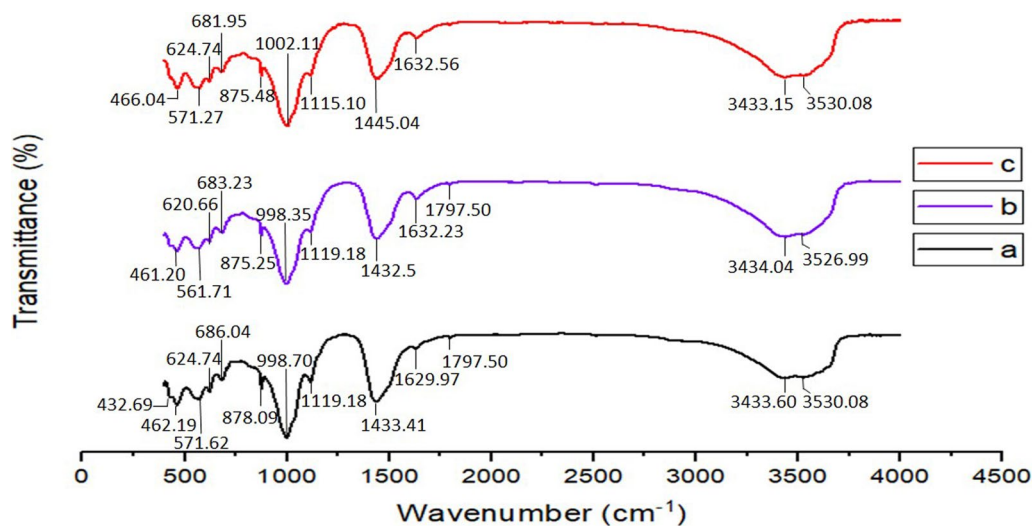


Fig. 2 FTIR spectrum of before (mud red a and modified mud red b) and after c adsorption

EDX, DLS, and zeta potential

EDX, DLS, and zeta potential analyses were used to determine the main elements, the size of adsorbent, and the effective electric charge on the adsorbent surface. Figure 3 shows the EDX analysis of MRM. According to the EDX image (Fig. 3), the composition of MRM was found to be 49.03% carbon, 32.13% oxygen, and 15.33% nitrogen. Table 2 displays DLS and zeta potential data for RM and MRM. According to Table 2, the average diameter of RM and MRM was found to be 1182 nm and 1202.9 nm, respectively.

The zeta potential shows the mechanism of electrostatic dispersion and the stability of the adsorbent particles relative to each other. If the adsorbent particles have a

significant positive or negative zeta potential ($\zeta > +30$ mV and $\zeta < -30$ mV), it can be concluded that the particles repel each other. There is dispersion stability. However, in the case of the minimal zeta potential (-30 mV $< \zeta < +30$ mV), there may be no significant force preventing aggregation of particles and instability of dispersion (Neolaka et al. 2022). From Table 2, the value of zeta potential for RM and MRM was -31.3 mV and -33.3 mV, respectively. Therefore, there is a stable dispersion between the adsorbent (Tor et al. 2009).

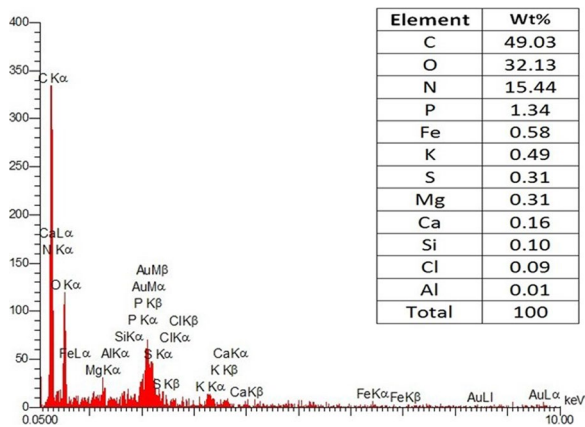


Fig. 3 EDX spectrum of modified mud red

Modeling of MDZ removal rate

The effect of main parameters, such as MRM dose, the initial MDZ concentration, the pH and the contact time on MDZ removal rate was investigated. The findings of MDZ removal by RM are exhibited in Table 3.

From Table 3, the removal efficiency of MDZ ranged from 26.25 to 69.87%. Table 4 exhibits the statistical adequacy assessment of models. Table 5 shows the coefficients of the quadratic model of MDZ removal.

According to Table 5, the quadratic model of MDZ elimination is displayed based on the parameters coded in Eq. 5:

$$R = + 67.04 - 5.77 A + 3.82 B + 1.98 C - 2.45 D + 8.21 AB + 0.7 AC + 0.94 AD - 1.88 BC + 4.91 BD + 2.11 CD - 18.18 A^2 - 6.94 B^2 - 5.74 C^2 - 11.24 D^2 \quad (5)$$

In this equation, each model has two variable and fixed sections. Accordingly, the removal rate was predicted to be 67.04%. The coded factors of A, B, C and D had the coefficients of -5.77, 3.82, 1.98 and -2.45 respectively. The factor of A with a coefficient of -5.77 had the maximum effect of MDZ removal. AB had the maximum interaction, and A² was the greatest square effect of the factors (Mazloomi et al. 2021).

Table 2 DLS and zeta potential for both for red mud and modified red mud

Factors (mV)	DLS				Zeta Potential
	Z-average (nm)	Mean (nm)	S.D. (nm)	Mode (nm)	
Red mud	1182	172	45.3	144.9	-31.3
Modified red mud	1202.9	94.1	25.4	78.5	-33.3

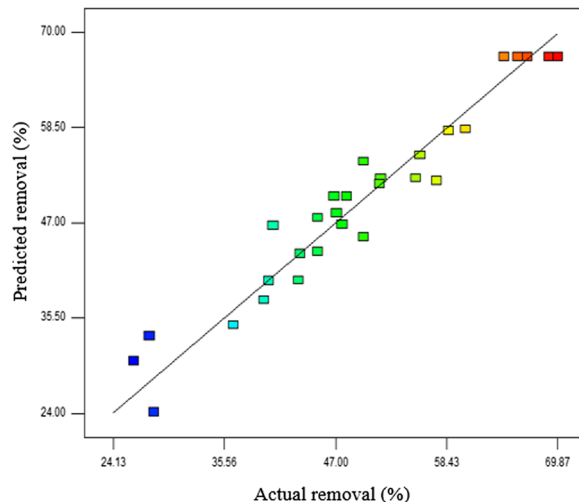


Fig. 4 Distribution of experimental vs. predicted removal for MDZ adsorption onto RM

Table 6 indicates analysis of variance (ANOVA) for quadratic model of MDZ removal using MRM. Overall, the findings of Table 6 was significant (*P*-value < 0.05). The values of R², predicted R², adjusted R² and adequacy precision were acquired to be 0.87, 0.27, 0.74 and 9.62, respectively.

From Table 6, MDZ removal rate is statistically significant. Figure 4 exhibits actual versus predicted removal. Based on Figure 4, the adequacy of the model to state a perfect prediction for MDZ removal is evident.

The effect of main parameters on MZD removal

Figure 5a–b demonstrates the relationship between the removal efficiency and the main parameters, including initial MDZ concentration, contact time, pH and MRM dose.

Initial antibiotic concentration and its effect

As can be seen from Fig. 5a, with increasing antibiotic concentration, the removal efficiency decreases (*P*-value < 0.05). The gradual decrease in removal efficiency may be attributed to the saturation of active sites on the adsorbent surface with metronidazole molecules at high pollutant concentrations, leaving no available sites for additional molecules to bind. At low concentrations, numerous active sites exist on the

Table 3 BBD matrix for MDZ removal using MRM

Run No.	Coded variable				Removal (%)	Run No.	Coded variable				Removal (%)
	A	B	C	D			A	B	C	D	
1	1	0	-1	-1	49.9	16	0	0	0	0	68.96
2	0	-1	-1	0	40.58	17	0	1	1	0	60.38
3	-1	0	-1	0	45.15	18	1	0	0	1	26.25
4	0	1	0	1	55.7	19	-1	0	1	0	46.86
5	0	0	-1	1	45.15	20	0	0	0	0	69.87
6	1	0	0	-1	27.86	21	0	0	0	0	64.35
7	1	0	1	0	43.16	22	-1	1	0	0	43.34
8	-1	-1	0	0	57.38	23	0	1	-1	0	58.62
9	-1	0	0	-1	47.69	24	0	1	0	-1	48.12
10	0	0	0	0	65.78	25	1	1	0	0	47.12
11	1	-1	0	0	28.32	26	0	0	1	-1	55.23
12	0	0	1	1	51.56	27	0	-1	0	-1	51.65
13	0	-1	1	0	49.85	28	-1	0	0	1	40.15
14	1	0	-1	0	36.47	29	0	0	0	0	66.75
15	0	-1	0	1	39.61						

Table 4 Statistical adequacy evaluation of models

Source	Sequential P-value	Lack of Fit P-value	Adjusted R ²	Predicted R ²
Linear	0.3164	0.0021	0.0346	-0.0927
2FI	0.8634	0.0014	-0.1327	-0.4509
Quadratic	<0.0001	0.0222	0.7438	0.2728
Cubic	0.0200	0.1659	0.9500	

surface of RM. The presence of metronidazole molecules attached to them results in a high removal efficiency (Fang et al. 2011). Fang et al. (2011) obtained similar results (Fang et al. 2011).

Contact time and its effect

The results of Fig. 5a showed that the antibiotic removal efficiency increases with increasing contact time (P-value < 0.05). This indicates that as the contact time increases, more MDZ molecules are gradually adsorbed on the active sites. This type of adsorption behavior is not uncommon and can be attributed to factors such as

Table 5 The coefficients of the quadratic model of MDZ removal

Factor	Coefficient estimate	df	Standard error	95% CI Low	95% CI High	VIF
Intercept	67.04	1	1.89	63.00	71.09	
A-Conc	-5.77	1	1.21	-8.37	-3.17	1.01
B-time	3.82	1	1.22	1.21	6.44	1.0000
C-Dose	1.98	1	1.22	-0.6409	4.61	1.01
D-pH	-2.45	1	1.22	-5.07	0.1761	1.01
AB	8.21	1	2.11	3.69	12.73	1.0000
AC	0.7092	1	2.09	-3.76	5.18	1.03
AD	0.9467	1	2.09	-3.53	5.42	1.03
BC	-1.88	1	2.11	-6.40	2.65	1.0000
BD	4.91	1	2.11	0.3821	9.43	1.0000
CD	2.11	1	2.14	-2.48	6.70	1.03
A ²	-18.18	1	1.67	-21.76	-14.60	1.08
B ²	-6.94	1	1.66	-10.50	-3.38	1.09
C ²	-5.74	1	1.66	-9.29	-2.19	1.08
D ²	-11.24	1	1.66	-14.79	-7.69	1.08

Table 6 ANOVA for quadratic model of MDZ removal by MRM

	Sum of Squares	df	Mean Square	F-value	P-value
Model	3697.15	14	264.08	14.85	<0.0001
A-Conc	402.50	1	402.50	22.63	0.0003
B-Time	175.49	1	175.49	9.87	0.0072
C-Dose	46.75	1	46.75	2.63	0.1273
D-pH	71.22	1	71.22	4.00	0.0652
AB	269.62	1	269.62	15.16	0.0016
AC	2.06	1	2.06	0.1156	0.7389
AD	3.66	1	3.66	0.2060	0.6569
BC	14.10	1	14.10	0.7927	0.3883
BD	96.24	1	96.24	5.41	0.0356
CD	17.25	1	17.25	0.9700	0.3414
A ²	2109.87	1	2109.87	118.61	<0.0001
B ²	310.60	1	310.60	17.46	0.0009
C ²	213.58	1	213.58	12.01	0.0038
D ²	820.28	1	820.28	46.12	<0.0001
Residual	249.03	14	17.79		
Lack of Fit	228.48	10	22.85	4.45	0.0817
Pure Error	20.55	4	5.14		
Cor Total	3946.17	28			
R ²	0.93		Predicted R ²	0.66	
Adjusted R ²	0.87		Adeq Precision	14.14	

the surface area, pore size, and chemical properties of the adsorbent. When MDZ molecules come into contact with the active sites on the surface of the adsorbent, they undergo a physical or chemical interaction, which leads to adsorption. The gradual increase in adsorption over time can be explained by the fact that as more MDZ molecules are adsorbed onto the active sites, fewer sites become available for further adsorption. As the number of available sites decreases, the adsorption rate also decreases. This results in a slower but continuous adsorption of the remaining MDZ molecules. Overall, these findings indicate that the adsorption process is effective in removing MDZ molecules from the solution. Increasing the contact time can lead to higher removal efficiency (Mohebbad et al. 2019).

The pH effect study

In the adsorption process, the pH of the solution can affect the functional groups in the adsorbent, the degree of ionization and the removal efficiency. Figure 5b shows that the MDZ removal rate was highest at a pH ranging from 5.5 to 8 (P -value > 0.05). At pH above 8 and below 5.5, the removal efficiency of MDZ decreased. On the other hand,

MDZ decreased in acidic pH due to the electrostatic repulsion between the adsorbent surface and MDZ-H⁺. At a pH higher than 8, the negative charge of the adsorbent surface and MDZ molecules led to a decreasing removal efficiency due to the repulsive electrostatic interactions. Therefore, the highest MDZ removal was expected at a pH around neutral or close to the point of zero charge of the adsorbent (Bonyadi et al. 2021).

Adsorbent dose effect

Based on the results of Fig. 5b, at the high dose of adsorbent, the maximum amount of MDZ removal was. In fact, with increasing adsorbent dose, the removal percentage increases (P -value > 0.05). The reason is that by increasing the adsorbent dose, a large accessible surface is provided for the surface adsorption process, and as a result, more molecules are attracted to the adsorbent surface. These findings are consistent with the study of Ahmadfazelizadeh et al. (2021).

Isotherm and kinetic models

Kinetic equations are used to explain the transfer behavior of adsorbed substance molecules per unit of time or to test the variables affecting the reaction rate (Movasaghi et al. 2019). In this research, pseudo-first-order, pseudo-second-order, and intraparticle diffusion kinetics were used to investigate the factors affecting reaction rate. Kinetic and isotherm parameters for MDZ removal are shown in Table 7. To know the application of kinetic and isotherm model, the correlation coefficient (R^2) was analyzed.

The values of the kinetic parameters of the Adsorption process of MDZ shows that the correlation coefficient (R^2) for the pseudo-first-order kinetics, pseudo-second-order kinetics, and intraparticle diffusion kinetics are $R^2 = 0.87$, $R^2 = 0.99$ and $R^2 = 0.96$, respectively. Based on this, the pseudo-second order equation with the correlation coefficient (R^2) is dominantly effective on the adsorption process. (Bonyadi et al. 2022a, b).

Adsorption isotherm models and equations are used to describe the properties of the adsorbent surface, providing useful information about the mechanism of the adsorption process. Adsorption isotherms are important factors in designing the adsorption system and describing the relationship between the concentration of adsorbed substances and the adsorption capacity of an adsorbent (Bonyadi et al. 2022a, b). Experimental equilibrium data was analyzed using isotherm models, including Langmuir, Freundlich and Temkin.

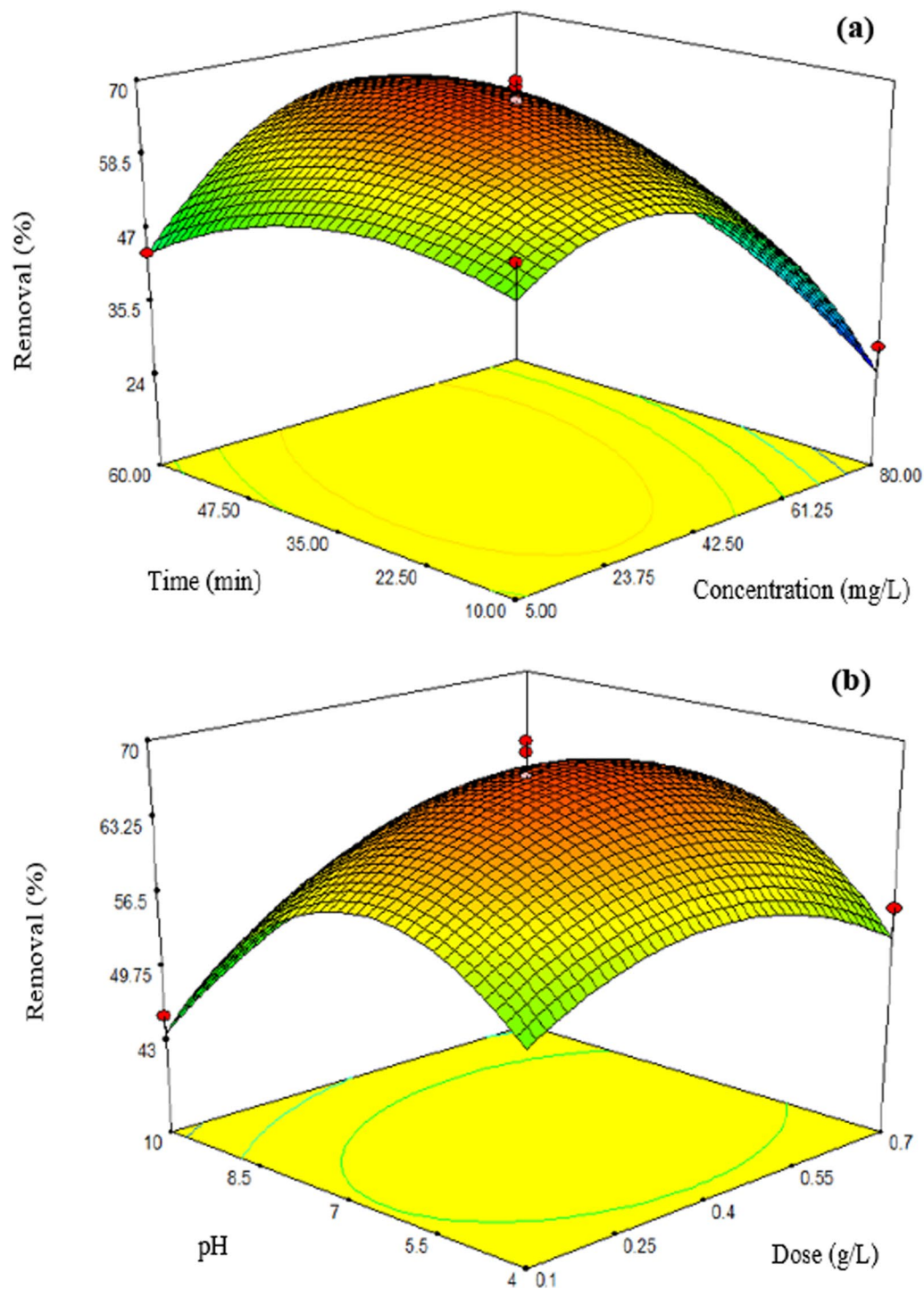


Fig. 5 Response surface plot about the effects of (a) Conc. vs. time, (b) Dose vs. pH

The results of this research had more consistent with the Langmuir isotherm ($R^2 = 0.99$) than the Freundlich and Tomkin isotherms. Following the adsorption process from the Langmuir model shows that MDZ is uniform and single-layered on MRM and all adsorbent surfaces

have the same energy in the adsorption process (Sepehr et al. 2017).

Table 8 shows the adsorption capacity of RM and other adsorbents used for MDZ removal. The data in Table 8 indicate that RM has a good potential to remove MDZ from aqueous solutions.

Table 7 The kinetic and isotherm parameters fitted for MDZ removal by MRM

Kinetic model	Linear form	Parameter	Value		
			20 mg L ⁻¹	40 mg L ⁻¹	80 mg L ⁻¹
Pseudo-first order	$\log(q_e - q_t) = \log q_e - \frac{k_1}{2.303} \cdot t$	$q_{e,cal}$ [mg/g]	0.97	1	-0.84
		K_1 [min ⁻¹]	0.29	1.84	0.03
		R^2	0.99	0.87	0.87
Pseudo-second order	$\frac{t}{q_t} = \frac{1}{k_2 q^2} + \frac{1}{q} \cdot t$	$q_{e,cal}$ [mg/g]	6.66	3.42	14.92
		K_2 [min ⁻¹]	0.02	0.38	-0.01
		R^2	0.99	0.92	0.99
Intra-particle diffusion	$qt = k_p \cdot t^{0.5} + c$	K_p [mg/g. min ^{-0.5}]	0.07	1.29	0.03
		R^2	0.96	0.78	0.26
Isotherm model	Linear form	Parameter	Value		
Langmuir	$\frac{C_e}{q_e} = \frac{1}{q_m} C_e + \frac{1}{q_m b}$	q_{max} (mg/g)	6.04		
		K_L (L/mg)	1.66		
		R^2	0.99		
Freundlich	$\text{Log } q_e = \log K_F + \frac{1}{n} \log C_e$	K_F mg/g(L/mg) ^{1/n}	28.49		
		N	0.71		
		R^2	0.86		
Temkin	$q_e = B_1 \ln k_t + B_1 \ln C_e$	k_t (L/mg)	1.11E+58		
		B_1	0.2		
		R^2	0.85		

Table 8 Comparison of Langmuir adsorption capacities of different adsorbents for MDZ

Adsorbent	Adsorbate TTC [mg g ⁻¹]	Reference
LECA	56.31	Kalhuri et al. (2017)
kaolin	41.32	Aleanizy et al. (2015)
Activated carbon	5.99	Belhassen et al. (2017)
Fe-modified sepiolite	5.62	Ding et al. (2015)
Red mud	6.04	Current study

Conclusion

In the present study, MRM was used to remove MDZ from aqueous environment. MRM was recognized as an effective, inexpensive and available adsorbent. Analysis of the adsorbent using FESEM, FTIR, EDX, DLS, and zeta potential provided valuable insights into its morphology, surface characteristics, functional groups, size, and

electrical charge. Acid modification of red mud increased the porosity and number of pores on the adsorbent surface, thereby enhancing its ability to adsorb the MDZ antibiotic. The FTIR spectrum displays various bands corresponding to different functional groups, such as O–H, si(Al)–O, Fe–O and carbonate groups. EDX analysis revealed that the composition of MRM includes carbon, oxygen, and nitrogen elements. The DLS and zeta potential data demonstrate the impact of particle size and electric charge of the adsorbent on the removal of MDZ. The optimization of MDZ removal was achieved using the Box–Benken model. The highest removal rate of MDZ was achieved under optimized parameters, including a pH of 7, a contact time of 35 min, an adsorbent dose of 0.4 g/L, and an initial MDZ concentration of 42.5 mg/L, resulting in a removal rate of 69.87%. The removal of MDZ followed the pseudo-second-order and Langmuir models. The maximum adsorption capacity for MDZ was 6.04 mg/g. The results showed that MRM significantly removes MDZ from aqueous solutions.

Acknowledgements Not applicable.

Authors' contributions FLG performed the experiments; MZA performed the experiments and wrote the paper; ZB wrote and edited the paper, and conceived and designed the experiments.

Funding The authors would like to thank the financial support provided by the Mashhad University of Medical Science (Iran) through the grant number of 991345.

Data availability All necessary data are included in the document.

Declarations

Conflict of interest The authors declare that they have no conflict of interests.

Ethical approval This article does not contain any studies with human participants or animals performed by any of the authors.

Open Access This article is licensed under a Creative Commons Attribution 4.0 International License, which permits use, sharing, adaptation, distribution and reproduction in any medium or format, as long as you give appropriate credit to the original author(s) and the source, provide a link to the Creative Commons licence, and indicate if changes were made. The images or other third party material in this article are included in the article's Creative Commons licence, unless indicated otherwise in a credit line to the material. If material is not included in the article's Creative Commons licence and your intended use is not permitted by statutory regulation or exceeds the permitted use, you will need to obtain permission directly from the copyright holder. To view a copy of this licence, visit <http://creativecommons.org/licenses/by/4.0/>.

References

- Ahmadfazeli A, Poureshgh Y, Rashtbari Y, Akbari H, Pourali P, Adibzadeh A (2021) Removal of metronidazole antibiotic from aqueous solution by ammonia-modified activated carbon: adsorption isotherm and kinetic study. *J Water Sanit Hyg Dev* 11(6):1083–1096
- Aleanizy FS, Alqahtani F, Al Gohary O, El Tahir E, Al Shalabi R (2015) Determination and characterization of metronidazole–kaolin interaction. *Saudi Pharm J* 23(2):167–176
- Aydin S, Aydin ME, Beduk F, Ulvi A (2019) Removal of antibiotics from aqueous solution by using magnetic Fe₃O₄/red mud-nanoparticles. *Sci Total Environ* 670:539–546
- Belhassen H, Ghorbel-Abid I, Rim L (2017) Removal of metronidazole from aqueous solution using activated carbon. *Eur J Chem* 8(3):310–313
- Berges J, Moles S, Ormad MP, Mosteo R, Gómez J (2021) Antibiotics removal from aquatic environments: adsorption of enrofloxacin, trimethoprim, sulfadiazine, and amoxicillin on vegetal powdered activated carbon. *Environ Sci Pollut Res* 28(7):8442–8452
- Bonyadi Z, Noghani F, Dehghan A, van der Hoek JP, Giannakoudakis DA, Ghadiri SK, Anastopoulos I, Sarkhosh M, Colmenares JC, Shams M (2021) Biomass-derived porous aminated graphitic nanosheets for removal of the pharmaceutical metronidazole: optimization of physicochemical features and exploration of process mechanisms. *Colloids Surf A Physicochem Eng Asp* 611:125791
- Bonyadi Z, Khatibi FS, Alipour F (2022a) Ultrasonic-assisted synthesis of Fe₃O₄ nanoparticles-loaded sawdust carbon for malachite green removal from aquatic solutions. *Appl Water Sci* 12(9):221
- Bonyadi Z, Nasoudari E, Ameri M, Ghavami V, Shams M, Sillanpää M (2022b) Biosorption of malachite green dye over *Spirulina platensis* mass: process modeling, factors optimization, kinetic, and isotherm studies. *Appl Water Sci* 12(7):1–11
- Bonyadi Z, Fouladi Z, Robatjazi A, Zahmatkesh Anbarani M (2023) Reactive red-141 removal from synthetic solutions by γ -Al₂O₃ nanoparticles: process modeling, kinetic, and isotherm studies. *Appl Water Sci* 13(2):52
- da Conceição FT, da Silva MSG, Menegário AA, Antunes MLP, Navarro GRB, Fernandes AM, Dorea C, Moruzzi RB (2021) Precipitation as the main mechanism for Cd (II), Pb (II) and Zn (II) removal from aqueous solutions using natural and activated forms of red mud. *Environ Adv* 4:100056
- Deihimi N, Irannajad M, Rezai B (2018) Characterization studies of red mud modification processes as adsorbent for enhancing ferricyanide removal. *J Environ Manag* 206:266–275
- Ding H, Bian G (2015) Adsorption of metronidazole in aqueous solution by Fe-modified sepiolite. *Desalin Water Treat* 55(6):1620–1628
- Esmaili Z, Barikbin B, Shams M, Alidadi H, Al-Musawi TJ, Bonyadi Z (2023) Biosorption of metronidazole using *Spirulina platensis* microalgae: process modeling, kinetic, thermodynamic, and isotherm studies. *Appl Water Sci* 13(2):63
- Fang Z, Chen J, Qiu X, Qiu X, Cheng W, Zhu L (2011) Effective removal of antibiotic metronidazole from water by nanoscale zero-valent iron particles. *Desalination* 268(1–3):60–67
- Gondi R, Kavitha S, Kannah RY, Karthikeyan OP, Kumar G, Tyagi VK, Banu JR (2022) Algal-based system for removal of emerging pollutants from wastewater: a review. *Bioresour Technol* 344:126245
- Gu S, Kang X, Wang L, Lichtfouse E, Wang C (2019) Clay mineral adsorbents for heavy metal removal from wastewater: a review. *Environ Chem Lett* 17(2):629–654
- Hena S, Gutierrez L, Croué J-P (2020) Removal of metronidazole from aqueous media by *C. vulgaris*. *J Hazard Mater* 384:121400
- Ighalo JO, Igwegbe CA, Adeniyi AG, Adeyanju CA, Ogunniyi S (2020) Mitigation of metronidazole pollution in aqueous media by adsorption: a review. *Environ Technol Rev* 9(1):137–148
- Juela DM (2021) Promising adsorptive materials derived from agricultural and industrial wastes for antibiotic removal: a comprehensive review. *Sep Purif Technol* 120286
- Kalhari EM, Al-Musawi TJ, Ghahramani E, Kazemian H, Zarrabi M (2017) Enhancement of the adsorption capacity of the light-weight expanded clay aggregate surface for the metronidazole antibiotic by coating with MgO nanoparticles: studies on the kinetic, isotherm, and effects of environmental parameters. *Chemosphere* 175:8–20
- Li L, Mao Y, Dong H, Wang Y, Xu L, Liu S, Xu Q, Qiang Z, Ji F (2022) The ultrafiltration process enhances antibiotic removal in the full-scale advanced treatment of drinking water. *Engineering* 8(1):69–76
- Lima VB, Goulart LA, Rocha RS, Steter JR, Lanza MR (2020) Degradation of antibiotic ciprofloxacin by different AOP systems using electrochemically generated hydrogen peroxide. *Chemosphere* 247:125807
- Mazloomi S, Bonyadi Z, Haghghat GA, Nourmoradi H, Soori MM, Eslami F (2021) Removal of methylene blue by *Saccharomyces cerevisiae*: process modelling and optimization. *Desalin Water Treat* 236:318–325
- Mohebbad B, Bonyadi Z, Dehghan AA, Rahmat MH (2019) Arsenic removal from aqueous solutions using *Saccharomyces cerevisiae*: kinetic and equilibrium study. *Environ Prog Sustain Energy* 38(s1):S398–S402
- Movasaghi Z, Yan B, Niu C (2019) Adsorption of ciprofloxacin from water by pretreated oat hulls: equilibrium, kinetic, and thermodynamic studies. *Ind Crop Prod* 127:237–250

- Mpelane S, Mketi N, Bingwa N, Nomngongo PN (2022) Synthesis of mesoporous iron oxide nanoparticles for adsorptive removal of levofloxacin from aqueous solutions: kinetics, isotherms, thermodynamics and mechanism. *Alex Eng J* 61(11):8457–8468
- Nadaroglu H, Kalkan E, Demir N (2010) Removal of copper from aqueous solution using red mud. *Desalin* 251(1–3):90–95
- Nasoudari E, Ameri M, Shams M, Ghavami V, Bonyadi Z (2021) The biosorption of Alizarin Red S by *Spirulina platensis*; process modelling, optimisation, kinetic and isotherm studies. *Int J Environ Anal Chem* 1–15
- Nasrollahi N, Vatanpour V, Khataee A (2022) Removal of antibiotics from wastewaters by membrane technology: limitations, successes, and future improvements. *Sci Total Environ* 156010
- Nasuhoglu D, Rodayan A, Berk D, Yargeau V (2012) Removal of the antibiotic levofloxacin (LEVO) in water by ozonation and TiO₂ photocatalysis. *Chem Eng J* 189:41–48
- Neolaka YA, Lawa Y, Naat J, Riwu AA, Mango AW, Darmokoeseomo H, Widyaningrum BA, Iqbal M, Kusuma HS (2022) Efficiency of activated natural zeolite-based magnetic composite (ANZ-Fe₃O₄) as a novel adsorbent for removal of Cr (VI) from wastewater. *J Mater Res Technol* 18:2896–2909
- Pirsaheb M, Khodadadi T, Bonyadi Z, Sharafi K, Khosravi T (2013) Evaluation of pesticide residues 2, 4-D, Atrazine and Alachlor concentration in drinking water well of Mahidasht district-Kermanshah, Iran, 2010–2011. *World Appl Sci J* 23(11):1530–1537
- Sepehr MN, Al-Musawi TJ, Ghahramani E, Kazemian H, Zarrabi M (2017) Adsorption performance of magnesium/aluminum layered double hydroxide nanoparticles for metronidazole from aqueous solution. *Arab J Chem* 10(5):611–623
- Shirzad-Siboni M, Jafari SJ, Giasi O, Kim I, Lee S-M, Yang J-K (2014) Removal of acid blue 113 and reactive black 5 dye from aqueous solutions by activated red mud. *J Ind Eng Chem* 20(4):1432–1437
- Smičiklas I, Smiljanić S, Perić-Grujić A, Šljivić-Ivanović M, Antonović D (2013) The influence of citrate anion on Ni (II) removal by raw red mud from aluminum industry. *Chem Eng J* 214:327–335
- Tandekar S, Korde S, Jugade R (2021) Red mud-chitosan microspheres for removal of coexistent anions of environmental significance from water bodies. *Carbohydr Polym Technol Appl* 2:100128
- Theamwong N, Intarabumrung W, Sangon S, Aintharabunya S, Ngernyen Y, Hunt AJ, Supanchaiyamat N (2021) Activated carbons from waste *Cassia bakeriana* seed pods as high-performance adsorbents for toxic anionic dye and ciprofloxacin antibiotic remediation. *Bioresour Technol* 341:125832
- Tor A, Cengeloglu Y, Aydin ME, Ersoz M (2006) Removal of phenol from aqueous phase by using neutralized red mud. *J Colloid Interface Sci* 300(2):498–503
- Tor A, Cengeloglu Y, Ersoz M (2009) Increasing the phenol adsorption capacity of neutralized red mud by application of acid activation procedure. *Desalination* 242(1–3):19–28
- Wang S, Boyjoo Y, Choueib A, Zhu Z (2005) Removal of dyes from aqueous solution using fly ash and red mud. *Water Res* 39(1):129–138
- Wang T, Pan X, Ben W, Wang J, Hou P, Qiang Z (2017) Adsorptive removal of antibiotics from water using magnetic ion exchange resin. *J Environ Sci* 52:111–117
- Weidner E, Siwińska-Ciesielczyk K, Moszyński D, Jesionowski T, Ciesielczyk F (2021) A comprehensive method for tetracycline removal using lanthanum-enriched titania-zirconia oxide system with tailored physicochemical properties. *Environ Technol Innov* 24:102016
- Yoosefian M, Ahmadzadeh S, Aghasi M, Dolatabadi M (2017) Optimization of electrocoagulation process for efficient removal of ciprofloxacin antibiotic using iron electrode; kinetic and isotherm studies of adsorption. *J Mol Liq* 225:544–553
- Zahmatkesh Anbarani M, Ramavandi B, Bonyadi Z (2023) Modification of *Chlorella vulgaris* carbon with Fe₃O₄ nanoparticles for tetracycline elimination from aqueous media. *Heliyon* 9(3)
- Zambrano J, García-Encina PA, Hernández F, Botero-Coy AM, Jiménez JJ, Irusta-Mata R (2021) Removal of a mixture of veterinary medicinal products by adsorption onto a *Scenedesmus almeriensis* microalgae-bacteria consortium. *J Water Process Eng* 43:102226
- Zhou R, Liu F, Du X, Zhang C, Yang C, Offiong N-A, Bi Y, Zeng W, Ren H (2022) Removal of metronidazole from wastewater by electrocoagulation with chloride ions electrolyte: the role of reactive chlorine species and process optimization. *Sep Purif Technol* 290:120799

Publisher's Note Springer Nature remains neutral with regard to jurisdictional claims in published maps and institutional affiliations.